MOLECULAR AND CELLULAR BIOLOGY, Feb. 1992, p. 563–575
0270-7306/92/020563-13$02.00/0

Vol. 12, No. 2

Characterization of Double-Strand Break-Induced Recombination: Homology Requirements and Single-Stranded DNA Formation

NEAL SUGAWARA AND JAMES E. HABER*

Rosenstiel Basic Medical Sciences Research Center and Department of Biology, Brandeis University, Waltham, Massachusetts 02254-9110

Received 30 July 1991/Accepted 6 November 1991

In the yeast *Saccharomyces cerevisiae*, a double-strand chromosome break created by the HO endonuclease is frequently repaired in mitotically growing cells by recombination between flanking homologous regions, producing a deletion. We showed that single-stranded regions were formed on both sides of the double-strand break prior to the formation of the product. The kinetics of the single-stranded DNA were monitored in strains with the recombination-deficient mutations *rad52* and *rad50* as well as in the wild-type strain. In *rad50* mutants, single-stranded DNA was generated at a slower rate than in the wild type, whereas *rad52* mutants generated single-stranded DNA at a faster rate. Product formation was largely blocked in the *rad52* mutant. In the *rad50 rad52* double mutant, the effects were superimposed in that the exonucleolytic activity was slowed but product formation was blocked. *rad50* appears to act before or at the same stage as *rad52*. We constructed strains containing two *ura3* segments on one side of the HO cut site and one *ura3* region on the other side to characterize how flanking repeats find each other. Deletions formed preterentially between the homologous regions closest to the double-strand break. By varying the size of the middle *ura3* segment, we determined that recombination initiated by a double-strand break requires a minimum homologous length between 63 and 89 bp. In these competition experiments, the frequency of recombination was dependent on the length of homology in an approximately linear manner.

Accumulating evidence indicates that the predominant process of double-strand break (DSB) repair in the yeast *Saccharomyces cerevisiae* involves homologous recombination. It has been suggested that free DNA ends find an intact homologous sequence and use it as a template for the repair of its sequence via DNA synthesis and ligation (57). This model is supported by a number of observations. Ionizing irradiation increases the number of unrepaired DNA DSBs in radiation-sensitive mutants that are also deficient in recombination functions (9, 58). Transformation experiments show that when linear DNA is transformed into yeast, the ends recombine with homologous chromosomal sequences (49). During meiosis, DSBs have been found near two known recombination hot spots and may be repaired by initiating recombination events (10, 71). Also, in *S. cerevisiae*, dicentric chromosomes generate broken chromosomes that appear to be healed by recombination (21, 22).

DSBs made in vivo by the HO endonuclease are also repaired via recombination. The DSB at the mating type locus, *MAT*, is formed by the HO endonuclease and is repaired by recombining with homologous sequences found at the silent cassettes, *HMR* or *HML* (30, 31, 43, 70). The DSB is lethal when it cannot be repaired in strains possessing deletions of *HMR* and *HML* or in recombination-defective *rad52* strains (27, 35, 54, 77, 78). A number of studies have moved the HO cut site from the *MAT* locus to other genomic locations and have shown that the DSB will stimulate recombination between homologs mitotically, meiotically (29, 55), and ectopically (55). A DSB located within a repeated sequence can stimulate recombination between the repeats (16, 47, 48, 51, 56, 64).

The HO endonuclease will also stimulate repair processes when the HO cut site is embedded in unique sequences and flanked by repeated sequences (48, 56, 63). A specific example of this process is examined further in this paper and is diagrammed in Fig. 1 (63). In this experiment, the HO cut site was integrated into the chromosome between repeated *ura3* sequences. The HO endonuclease was placed under the control of a galactose-inducible promoter. When HO was induced, the cut site was cleaved and the two repeated sequences recombined to form one copy of *ura3*. This recombination event resulted in the deletion of the intervening sequences and the process could be monitored by Southern blots.

We investigated the fates of the DNA ends after DSB formation by examining whether single-stranded regions were formed near the DSB. Single-stranded DNA (ssDNA) may play a role in the formation of heteroduplex structures either by strand invasion (24, 46, 73) or by annealing of the single-stranded regions of homology (32). In *S. cerevisiae*, evidence that ssDNA is involved during recombination processes is provided by experiments examining DSBs formed during meiosis at *ARG4* (71, 72) and during mating type switching (78). When HO endonuclease cuts *MAT*, ssDNA forms, leaving a 3′ tail on only the right side of the DSB. A greater amount of ssDNA is formed in *rad52* mutants and in strains lacking the donor cassettes, *HMR* and *HML*. Also, in the strains deleted for *HMR* and *HML*, the left side is no longer protected such that ssDNA is formed on both sides of the cut site (78). Single-stranded recombination intermediates also form when DNA is injected into *Xenopus* oocytes (11, 39–41).

We also explored the homology requirements for mitotic recombination initiated by a DSB. With respect to spontaneous recombination in which the nature of the initiating event is not known, the frequency of recombination is dependent on the length of homology in several organisms. Decreasing the regions of homology decreases the frequency of recombination in a linear manner. This is seen in the T4

* Corresponding author.

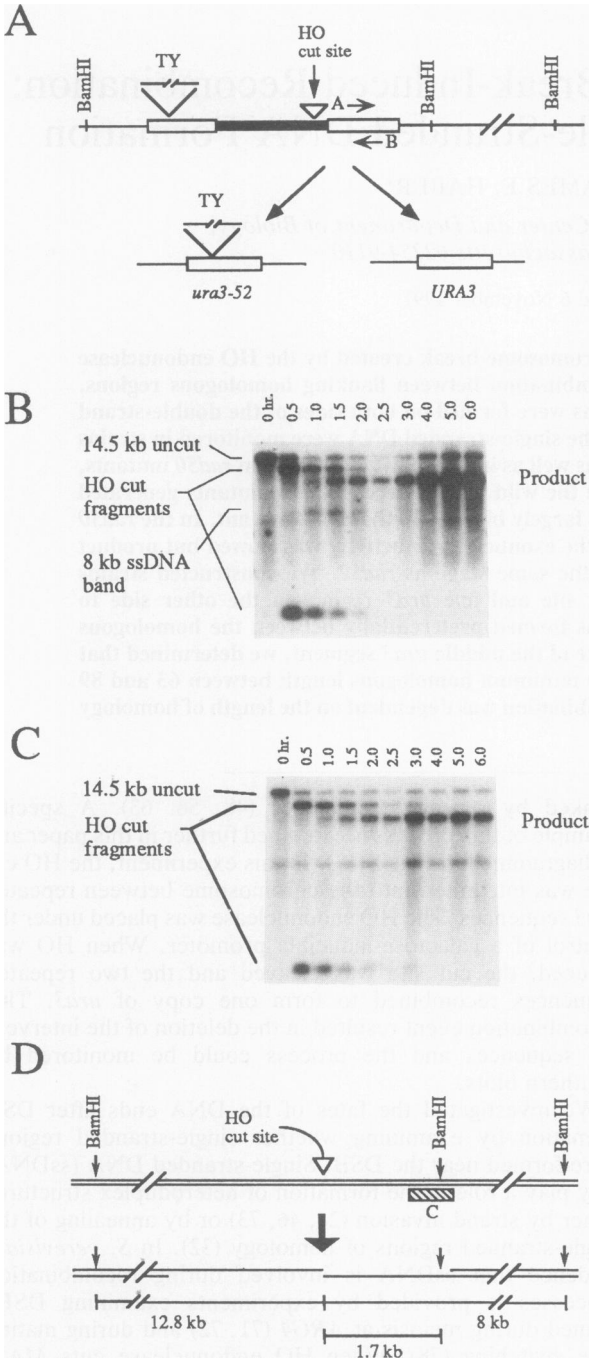

FIG. 1. DSB initiates the formation of ssDNA and recombination between flanking repeats. (A) The HO cut site was located in pUC9 sequences (dark line) between two *ura3* sequences (open boxes) in tNR111. The *ura3-52* sequence on the left contains a 6-kb TY element inserted into the coding region (61). The HO-initiated DSB caused the *ura3* sequences to recombine to form two structures: a *ura3-52* allele if recombination occurred to the right of the TY element or a *URA3* allele if the sequences recombined to the left of the TY element. The letters A and B at *ura3* indicate riboprobes complementary to the bottom and top strands of DNA, respectively. Horizontal arrows show the direction of transcription. (B) HO was induced in tRN111, and DNA samples from the time points shown were digested with *Bam*HI, electrophoresed in a denaturing gel, blotted, and probed with the *ura3* riboprobe A. Lane 1 (0 hr.) shows the 14.5-kb *Bam*HI fragment before cutting by the HO endonuclease. Lane 2 (0.5 h) shows the two HO-cut fragments, 12.8 kb and 1.7 kb, to the left and right of the DSB, respectively. The ssDNA 8-kb band appeared by 30 min and disappeared by 3 h. The 7.3-kb band in all the lanes in panels B and C was likely due to a small amount of read-through riboprobe transcript hybridizing to sequences from pSE271::GAL10::HO. (C) The Southern blot was prepared as described above with the same time course DNA. The blot was probed with riboprobe B. The 8-kb ssDNA band was not detected. (D) Restriction map, showing the origin of the ssDNA. An exonucleolytic activity degraded one strand past the first *Bam*HI site located 1.7 kb away from the HO cut site. *Bam*HI failed to cut the ssDNA, resulting in a larger 8-kb *Bam*HI fragment. Box C shows the location of a DNA probe (see text).

phage, *Escherichia coli*, and most mammalian cell lines examined (5, 33, 34, 62, 67, 69, 76). Only two cases of a nonlinear dependence were reported. One is in a cell line in which plasmid recombination frequencies were measured (5). In the other case, a logarithmic relationship was found when rates of spontaneous recombination were measured between inverted *his3* alleles on a plasmid in *S. cerevisiae* (2). In a different experimental design but also in *S. cerevisiae*, Yuan and Keil found that recombination rates leveled off with lengths greater than 1 kb (80). We were interested in determining whether an HO-induced DSB created in a unique sequence would induce recombination between flanking repeats with a linear, logarithmic, or other dependence on homology. We also wished to determine what the minimum homology requirements would be. The minimal length for efficient spontaneous recombination in other organisms ranged from 23 to 300 bp (5, 33, 67, 69, 76).

This study also examines the effects of the *rad50* and *rad52* mutations on DSB-induced recombination to better understand their roles. *rad50* and *rad52* confer sensitivity to ionizing radiation and are deficient in meiotic recombination (8, 17, 36, 37, 53). *rad52* mutants are also defective in mitotic recombination (23, 36, 38, 53), mating type switching (27, 35, 77, 78), intrachromosomal gene conversion (26, 28), and the repair of HO-induced breaks (48, 63, 78). When a DSB is made by the HO endonuclease or by I-SceI (a mitochondrial endonuclease from *S. cerevisiae*), mitotic recombination between direct repeats on a plasmid is reduced by 90% in *rad52* strains (16, 51). An exception occurs in the rDNA repeated array, in which mitotic recombination is not reduced in a *rad52* mutant (52, 81) and in which HO-induced DSBs within the rDNA are efficiently repaired (50).

The *rad50* mutant differs from the *rad52* mutant in several respects. It is less sensitive than the *rad52* mutant to ionizing radiation (44). It exhibits a mitotic hyper-Rec phenotype at some loci both inter- and intrachromosomally (20, 37) and is not absolutely essential for mating type switching (36) or HO-induced recombination (15, 78). In combination, the *rad50 rad52* double mutant exhibits the sensitivity to ionizing radiation of *rad52*, i.e., *rad52* is epistatic to *rad50* (44). *rad52* is also epistatic to *rad50* with respect to spontaneous mitotic recombination (36). The efficiency of HO-induced recombination in the experiments described here allows us to examine the effects of the single and combined mutations on recombination in a detailed manner by use of Southern blots and by hybridization of single-stranded probes to potential ssDNA intermediate structures.

MATERIALS AND METHODS

Plasmids. pNR6 (63) contains the 117-bp HO cut site of *MAT***a** inserted between the *Hin*cII and *Bam*HI sites of

pUC9 and the *URA3* 1.17-kb *Hin*dIII fragment at the *Hin*dIII site transcribed away from the HO cut site. pNSU102 was created by filling in the downstream *Hin*dIII site and inserting the 2.3-kb *Hin*dIII fragment from lambda phage into the upstream *Hin*dIII site.

The deletions of *ura3* sequences were constructed by first inserting *Bgl*II or *Bam*HI linkers into the *ura3* sequence at the *Nde*I, *Pst*I, *Eco*RV, or *Alw*NI site of pHS113. pHS113 contains the *URA3* 1.17-kb fragment with *Bam*HI linkers in the plasmid pMLC28 (B. Seed). Linker insertions into *ura3* were carried out as described by Seth (66). The appropriate *Bam*HI-*Bgl*II and *Bam*HI *ura3* restriction fragments were cloned into the *Bam*HI site of pNSU118. pNSU118 has the same structure as pNSU102 except that *Bam*HI linkers were inserted at the unique *Nar*I site (filled in). pNSU126, pNSU122, pNSU123, pNSU128, and pNSU119 contain direct duplications of 142, 205, 415, 905, and 1,170 bp, respectively, of *ura3* sequences from the 5′ end. In addition to the 5′ *ura3* fragments discussed above, the 136-bp *Hin*cII internal fragment of *ura3* was ligated into the filled-in *Bam*HI site of pNSU118 to yield pNSU138. Also, the 262-bp *Alw*NI fragment (filled in and ligated to *Bam*HI linkers) from the 3′ end of *ura3* was cloned into the *Bam*HI site of pNSU102 to give pNSU135.

Plasmids containing the 30, 63, or 89 bp of *ura3* were constructed by first ligating the annealed oligonucleotides gatcggccatataggccTGTTGAAGAAACATGAAATTGCCC AGTATTtg and gatccaaATACTGGGCAATTTCATGTTTC TTCAACAggcctatatggcc into the *Bam*HI site of pNSU118, destroying the *Bam*HI site at the 5′ end. pNSU141 possessed 30 bp of duplicated *ura3* sequence (capital letters). Flanking sequences provided restriction sites to facilitate subsequent constructions. The 5′-flanking sequence contains an *Sfi*I site, and the 3′ sequence contains a *Pfl*MI site, each possessing compatible sticky ends when cleaved. pNSU141 was cleaved with *Sfi*I and *Bam*HI and ligated to the annealed oligonucleotides gatCTTTCGACATGATTTATCTTCGTT TCCTGCAGGTTTTTGTTCTGTGCAGTTGGGTTAAG AATA and TCTTAACCCAACTGCACAGAACAAAAACC TGCAGGAAACGAAGATAAATCATGTCGAAA, yielding pNSU146 with 63 bp of *ura3*. pNSU141 was also cut with *Pfl*MI and *Bam*HI and ligated to the latter pair of annealed oligonucleotides to give a combined 89 bp of *ura3* in the plasmid pNSU147. The sequence of the *Pfl*MI site and the *ura3* sequences were chosen to result in 89 bp of a continuous *ura3* sequence. The sequences of the 30-, 63-, and 89-bp *ura3* sequences (as well as the 136 bp of *ura3* in pNSU138) were confirmed by DNA sequencing.

A *rad52* gene disruption was created by ligating the *THR4* gene contained on a 3-kb *Hin*dIII fragment (end filled) from p323 (G. Simchen) into the *RAD52* gene in pSM13 (65) between the two *Asp*718 sites (also end filled). This replaces 353 bp of the *rad52* reading frame (1) with the *THR4* disruption in the resulting plasmid, pNSU165.

pNSU160 was constructed by deleting the *Pst*I fragments from pNSU146, resulting in a single copy of *ura3* deleted for the first 173 bp from the beginning of the 1.17-kb *ura3* *Hin*dIII fragment. The *TRP1 ARS1 Nhe*I fragment from YRp7 was ligated into the *Nhe*I site, resulting in pNSU161.

pSE271::GAL10::HO is a GAL10::HO fusion cloned into a *TRP1 ARS1 CEN4* vector (F. Heffron). pRHB73 contains *TRP1* and a *ura3-Nco*I allele (with the *Nco*I site filled in) (R. Borts). pSK180 contains the 13-kb *Eco*RI fragment encompassing the *URA3* gene (60).

TABLE 1. Strains

Strain(s)	Genotype
R167	*ho HMLα matΔ::LEU2 hmr-3Δ mla2 thr trp1 leu2 ura3 GAL*$^+$ pGalHO (*Gal10::HO URA3 CEN4 ARS1*)
tNR85	*ho HMLα leu2 matΔ::LEU2 hmr-3Δ mal2 ura3-52 trp1 thr GAL*$^+$ pSE271::GAL10::HO (*TRP1 ARS1 CEN4*)
tNR111	tNR85::pNR6 (*ura3-52* cut site *URA3*)[a]
tNS24	tNR85::pNSU102 (*ura3-52* cut site *URA3*)
tNS38	*ho HMLα matΔ::LEU2 hmr-3Δ mal2 thr4 trp1 leu2 ura3 GAL*$^+$ *rad50::hisG* pSE271::GAL10::HO (*TRP1 ARS1 CEN4*)
tNS62	tNR85::pNSU122 (*ura3-52 ura3* (205 bp) cut site *URA3*)
tNS65	*ho HMLα matΔ::LEU2 hmr-3Δ mal2 thr4 trp1 leu2 ura3 GAL*$^+$ *rad50::hisG ura3-52* pSE271::GAL10::HO (*TRP1 ARS1 CEN4*)
tNS77	tNR85::pNSU123 (*ura3-52 ura3* (415 bp) cut site *URA3*)
tNS125	tNR85::pNSU126 (*ura3-52 ura3* (142 bp) cut site *URA3*)
tNS130, tNS362	tNR85::pNSU119 (*ura3-52 ura3* (1,170 bp) cut site *URA3*)
tNS224	tNR85::pNSU128 (*ura3-52 ura3* (905 bp) cut site *URA3*)
tNS228	tNR85::pNSU138 (*ura3-52 ura3* (136 bp) cut site *URA3*)
tNS247	tNR85::pNSU141 (*ura3-52 ura3* (30 bp) cut site *URA3*)
tNS262	tNR85::pNSU135 (*ura3-52 ura3* (262 bp) cut site *URA3*)
tNS267	tNR85::pNSU146 (*ura3-52 ura3* (63 bp) cut site *URA3*)
tNS275	tNR85::pNSU147 (*ura3-52 ura3* (89 bp) cut site *URA3*)
tNS313	tNS65::pNSU102 (*ura3-52* cut site *URA3*)
tNS324	*ho HMLα leu2 matΔ::LEU2 hmr-3Δ mal2 trp1 thr4 GAL*$^+$ pNSU119 (*ura3-Nco* cut site *URA3* (1,170 bp) URA3) pSE271::GAL10::HO (*TRP1 ARS1 CEN4*)
tNS327	*ho HMLα leu2 matΔ::LEU2 hmr-3Δ mal2 trp1 thr4 GAL*$^+$ pNSU119 (*ura3-Nco URA3* (1,170 bp) cut site *URA3*) pSE271::GAL10::HO (*TRP1 ARS1 CEN4*)
tNS351, tNS352	tNR85::pNSU119 (*ura3-52* cut site *URA3* (1,170 bp) *URA3*)
tNS397	*ho HMLα matΔ::LEU2 hmr-3Δ* (*ura3-52* cut site *URA3*) *mal2 thr4 trp1 leu2 ura3 GAL*$^+$ *rad50::hisG rad52::THR4* pSE271::GAL10::HO (*TRP1 ARS1 CEN4*)
tNS418	*ho HMLα matΔ::LEU2 hmr-3Δ* (*ura3-52* cut site *URA3*) *mal2 thr4 trp1 leu2 ura3 GAL*$^+$ *rad52::THR4* pSE271::GAL10::HO (*TRP1 ARS1 CEN4*)
tPSA4	*ho HMLα matΔ::LEU2 hmr-3Δ mal2 thr4 trp1 leu2 ura3 GAL*$^+$ *rad50::hisG::URA3::hisG*
tPSB5	*ho HMLα matΔ::LEU2 hmr-3Δ mal2 thr4 trp1 leu2 ura3 GAL*$^+$ *rad50::hisG* pNR6 (*ura3-52* cut site *URA3*)

[a] Cut site indicates the 117-bp *Bgl*II-*Hin*dIII *MAT***a** HO endonuclease recognition site inserted into pUC9 (see Materials and Methods).

Riboprobes were made from plasmids having the relevant sequences inserted into pGEM7Zf+ (Promega), pBluescript KS− (Stratagene), or pST54 (S. Tabor).

Strains. Strain genotypes are given in Table 1. Targeted integrations of plasmids into the *ura3-52* allele were accom-

plished by cleaving the relevant plasmid at either the unique *Stu*I or *Nco*I site in the *ura3* sequence and then by transformation into tNR85 (63) or tNS65. Since pNSU119 and pNSU128 each contain two *Stu*I sites, the linear form was gel purified from a partial *Stu*I digest prior to transformation.

A *rad50* strain (tPSA4) was constructed by transforming R167 with a *hisG*::*URA3*::*hisG* disruption of *rad50* from pNKY83 (3). A Ura$^-$ derivative was subsequently selected by its resistance to 5-fluoro-orotic acid (7) to give a *rad50*::*hisG* disruption. pNR6 was integrated into the *ura3-52* locus of tPSA4 to give tPSB5. pSE271::GAL10::HO was transformed into tPSB5 to yield tNS38. Galactose induction of tNS38 resulted in a Ura$^-$ derivative that retained the *ura3-52* allele. Subsequent *rad50* strain constructions utilized this derivative, tNS65. tNS65 was transformed with pNSU102 and targeted to *ura3-52* by digestion with *Stu*I to give tNS313.

The *rad52* disruptions in tNS397 and tNS418 were obtained by transformation of the 5-kb *Bam*HI fragment from pNSU165 into tNS313 and tNS24, respectively.

The TY52 element (61) at *ura3* was removed from tNR111 by inducing the strain with galactose and isolating a Ura$^+$ derivative that had lost the TY element as confirmed by Southern blots. A Trp$^-$ segregant (lacking pSE271::GAL10::HO) was isolated. pRHB73 (containing *TRP1* and the *Nco*I$^-$ allele of *ura3*) was cut with *Stu*I and integrated at the *ura3* locus by selecting for *TRP1*. Ura$^-$ derivatives were screened by Southern blots for retention of the *Nco*I$^-$ mutation. This strain was sequentially transformed with pSE271::GAL10::HO and pNSU119 (the linear form of a *Stu*I partial digest) to result in strains tNS324 and tNS327. Transformations were carried out with lithium acetate (25) or by electroporation (59).

Southern blots. Genomic DNAs of transformants were prepared by the SDS-potassium acetate method of Sherman et al. (68). Alkaline denaturing gels were run as described by McDonnel et al. (42). Southern blot hybridizations were carried out by the method of Church and Gilbert (13). DNA probes were prepared by the method of Feinberg and Vogelstein (14). RNA probes were prepared by the method of Melton et al. (45) as modified by Promega. Dot blots and Southern blots were scanned densitometrically by using β-particle scanners (the Betascope 603 blot analyzer [Betagen] or Ambis radioanalytic imaging system) or a Bio-Rad model 620 video densitometer.

ssDNA dot blot assay. The ssDNA dot blot assay was based on a principle used to detect ssDNA by Southern hybridization analysis (71, 72, 74). Native genomic DNA samples (1 μg per sample) were prepared in a 10× SSC solution (1× SSC is 0.15 M NaCl plus 0.015 M sodium citrate), and denatured samples were prepared in a 0.4 N NaOH solution by using 10% of the DNA used for the native samples. Genomic samples and the controls were applied to a nylon membrane with a dot blot manifold. After application, the wells were rinsed with 10× SSC. The membrane was removed from the apparatus and air dried. Both neutral and positively charged membranes were used. DNA was UV cross-linked to the membranes and hybridized by the method of Church and Gilbert (13). Additional controls included denatured and native pUC or lambda DNAs, denatured R167u DNA (a segregant of R167 lacking the GAL::HO plasmid), and unlabeled RNA transcripts from both strands to evaluate the strand specificity of the riboprobes.

Galactose inductions. Rich medium (YPD), nonfermentable (YP-lactate), and selective media (SD) were described by Rudin and Haber (63) and Sherman et al. (68). Strains were grown in YP-lactate medium, and HO was induced with 2% galactose, as described by Rudin and Haber (63). DNA samples were prepared according to the glass bead protocol (63). For overnight time point samples, the final aliquot was centrifuged, resuspended in sterile water, and incubated overnight at 30°C to allow recombination to continue while inhibiting cell growth.

Homology requirements. Strains were induced with galactose as described above. DNA samples were taken before induction and after 5 h of induction. DNA samples were digested with *Bgl*II, electrophoresed on a 0.5% agarose gel in 1× TAE buffer, blotted, and probed with a sequence downstream of *URA3* (the 1.2-kb *Hin*dIII-*Bgl*II fragment derived from pSK180) (60). Complete deletion products have a 2.9-kb band. Partial deletion products have a 5.6- to 6.6-kb band depending on the strain. Densitometry was carried out with a β-particle scanner. The fraction of partial deletions was calculated as the intensity of the partial deletion product over the sum of intensities of the partial and complete products after correcting for background. At the same time points, cells were plated onto SD-Trp or YPD. Colonies were replica plated onto selective media to determine the Ura and Trp phenotypes. The fraction of partial deletion product formed was the number of Ura$^+$ Trp$^+$ colonies divided by the number of Trp$^+$ colonies (possessing pSE271::GAL10::HO). Except for the strains tNS247, tNS267, and tNS275, no attempt was made to correct for uninduced cells or for cells that lost the TY element because of recombination, both of which are Ura$^+$. These events composed no more than 3% of the Trp$^+$ cells.

Partial deletion products arose at a low frequency in tNS247, tNS267, and tNS275, making it necessary to identify the uninduced colonies and TY-less recombinants. Individual colonies were initially analyzed by Southern blots by using *Bgl*II as described above, but subsequently colonies were scored by running uncut DNA on gels. In the latter approach, two identical Southern blots were probed with pUC19 or lambda sequences to identify which sequences remained in the chromosomal band. This process distinguished all possible recombinants. Only the Ura$^+$ colonies were examined by Southern blots after a 5-h induction.

Since the 63- and 89-bp *ura3* sequences [*ura3* (63 bp) and *ura3* (89 bp)] were not derived from the extreme 5′ end of the *ura3* *Hin*dIII fragment, it was necessary to determine whether the partial deletion product would possess a Ura$^+$ phenotype. We determined that the *ura3* (63 bp) fragment would give rise to a Ura$^+$ partial deletion product by transforming pNSU161 into a Trp$^-$ segregant of tNR85 to give tNS345. Mitotic segregants of tNS345 that were Trp$^+$ were also Ura$^+$. The *ura3* (89 bp) allele gave a partial deletion product, as determined from the Southern blots (*Bgl*II digests) described above, that was Ura$^+$. Since the *ura3* (30 bp) segment begins at the same nucleotide as the *ura3* (89 bp) sequence, it should also give rise to a partial deletion product that is Ura$^+$.

RESULTS

Single-stranded DNA is formed during DSB-initiated recombination between two repeated sequences. We wished to determine whether a 5′-to-3′ exonuclease acts at the HO cut site when the cut site is removed from the context of the *MAT* locus. In this case, the HO cut site was integrated as part of a plasmid into the *ura3* locus (Fig. 1) (63). Galactose-induced expression of HO caused the *ura3* sequences to

recombine in more than 97% of the cells possessing the GAL10::HO plasmid. This resulted in a Ura$^-$ phenotype since most recombination events occurred to the right of the TY element, leaving a *ura3*-52 allele. Those cells that remained Ura$^+$ had structures that recombined on the left side of the TY element or remained uninduced. Upon HO induction, the processing of the DSB and formation of the product could be clearly monitored on Southern blots (Fig. 1A), as previously shown by Rudin and Haber (63). DNA was isolated from cells at time points after the induction of HO, digested with *Bam*HI, and then run on a denaturing gel. After hybridization of the Southern blot with *ura3*, the autoradiogram showed the original 14.5-kb *Bam*HI fragment in the initial time point and two HO cut fragments appearing within 30 min. These two fragments disappeared as they were processed into a deletion product that started to appear at 1 h postinduction. In addition, a faint 8-kb band that has the kinetics of a potential intermediate in this process was observed. The 8-kb band appeared after DNA cleavage by HO endonuclease and disappeared as the product formed.

A test of whether this 8-kb band was a single-stranded structure was carried out by probing the blot with RNA probes to *URA3*. When one RNA strand was used as a probe (Fig. 1, probe A), hybridization to the 8-kb fragment was observed. There was no hybridization to this fragment when the complementary strand was used as a probe (Fig. 1B and C). This indicates that the exonuclease leaves a single DNA strand with a 3′-to-5′ polarity. Hence, the exonuclease acts in a 5′-to-3′ direction, leaving a 3′ tail at the cut site. The 8-kb DNA fragment arose as a result of exonucleolytic degradation of one strand past the nearest *Bam*HI site, 1.7 kb from the HO cut site (Fig. 1D). The *Bam*HI site was lost, resulting in a larger restriction fragment. Upon reprobing with a sequence downstream of *URA3* (Fig. 1D, probe C), the probe hybridized to the 8-kb band, confirming its origin (not shown).

A denaturing gel was used to separate the strands to allow the 8-kb ssDNA fragment to migrate as a discrete band. This band did not appear in native gels because its partially single-stranded structure would cause it to run as a diffuse smear. Also, the exonuclease may act asynchronously or processively, resulting in a population of fragments with single-stranded regions heterogeneous in size. Since the transient intermediate comprises a small portion of the total DNA, the smearing could render the band undetectable. Furthermore, as longer regions of DNA become single stranded, higher-molecular-weight fragments are created. These may be difficult to visualize and quantitate on gels if they are extremely long.

Dot blot analysis of ssDNA formation. Given the complex nature of this analysis, it was desirable to develop a more direct method to identify and quantitate ssDNA near the HO cut site. For this purpose, we employed dot blots to avoid problems encountered in detecting and quantitating heterogeneously sized DNA on gels. In this method, time course genomic DNA was directly dot blotted onto nylon membranes without denaturation (see Materials and Methods) (71, 74). Under these conditions, ssDNA and some double-stranded DNA (dsDNA) binds to the membrane. The membrane was probed with RNA probes that hybridized preferentially to the ssDNA, thereby providing a sensitive means to measure the amount of ssDNA formed during a time course. As positive controls, the same genomic DNA samples were denatured and bound to the membrane by using only 1/10 the amount used in the native samples.

Figure 2 shows such an experiment using a strain in which the HO cut site was embedded between pUC9 and lambda phage sequences and flanked by *ura3* repeats. Upon cutting by the HO endonuclease, this structure efficiently recombined between the *ura3* sequences to yield a deletion product as shown by Southern blot analysis (Fig. 3A). The dot blot assay detected a very low signal, if any, in the 0-h time point prior to HO cutting (Fig. 2B). After HO induction, there was a significant increase in ssDNA formation that was absent when a probe of the complementary strand was used (Fig. 2C). Upon longer exposure, a weak and short-lived signal could be detected at the 15-min time point when the latter probe was used. The weak signal may have resulted from a weak nucleolytic activity that initiated degradation of the 3′ strand before the 5′ strand or from an unwinding of HO-cut DNA that was not renatured during DNA isolation.

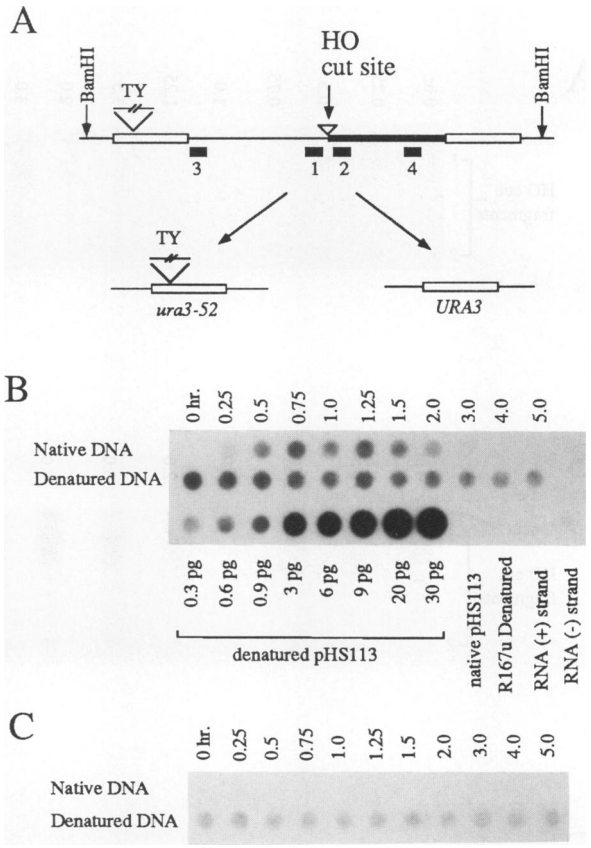

FIG. 2. ssDNA is formed on both sides of the HO cut site. (A) The HO cut site was flanked by *URA3* and *ura3-52* alleles (open boxes) in tNS24. Riboprobes (black boxes) 1 and 3 are pUC sequences (thin lines); riboprobes 2 and 4 are lambda phage sequences (dark line). Upon HO endonuclease cutting, the structure recombined to form *ura3-52* or *URA3*. (B) Time course samples were dotted onto membranes and probed with riboprobe 1 complementary to the strand ending 3′ at the DSB (the time points after induction are shown). Native DNA samples are from tNS24. Denatured samples were the same as the native DNA samples except that they were alkali denatured and only 1/10 of the DNA in the native samples was loaded. Bottom row: wells 1 to 8 (from left to right), denatured pHS113 loaded in the amounts of hybridizable sequence shown; well 9, 0.6 pg of nondenatured pHS113 DNA; well 10, 0.5 μg of denatured R167u (lacks pUC9 and lambda sequences); well 11, 0.1 pg of unlabeled RNA transcribed from DNA segment I; well 12, 0.1 pg of RNA (−) segment 1 transcribed to the right. (C) DNA was loaded as in panel B except that the blot was probed with the opposite strand (probe 1, transcribed to the right).

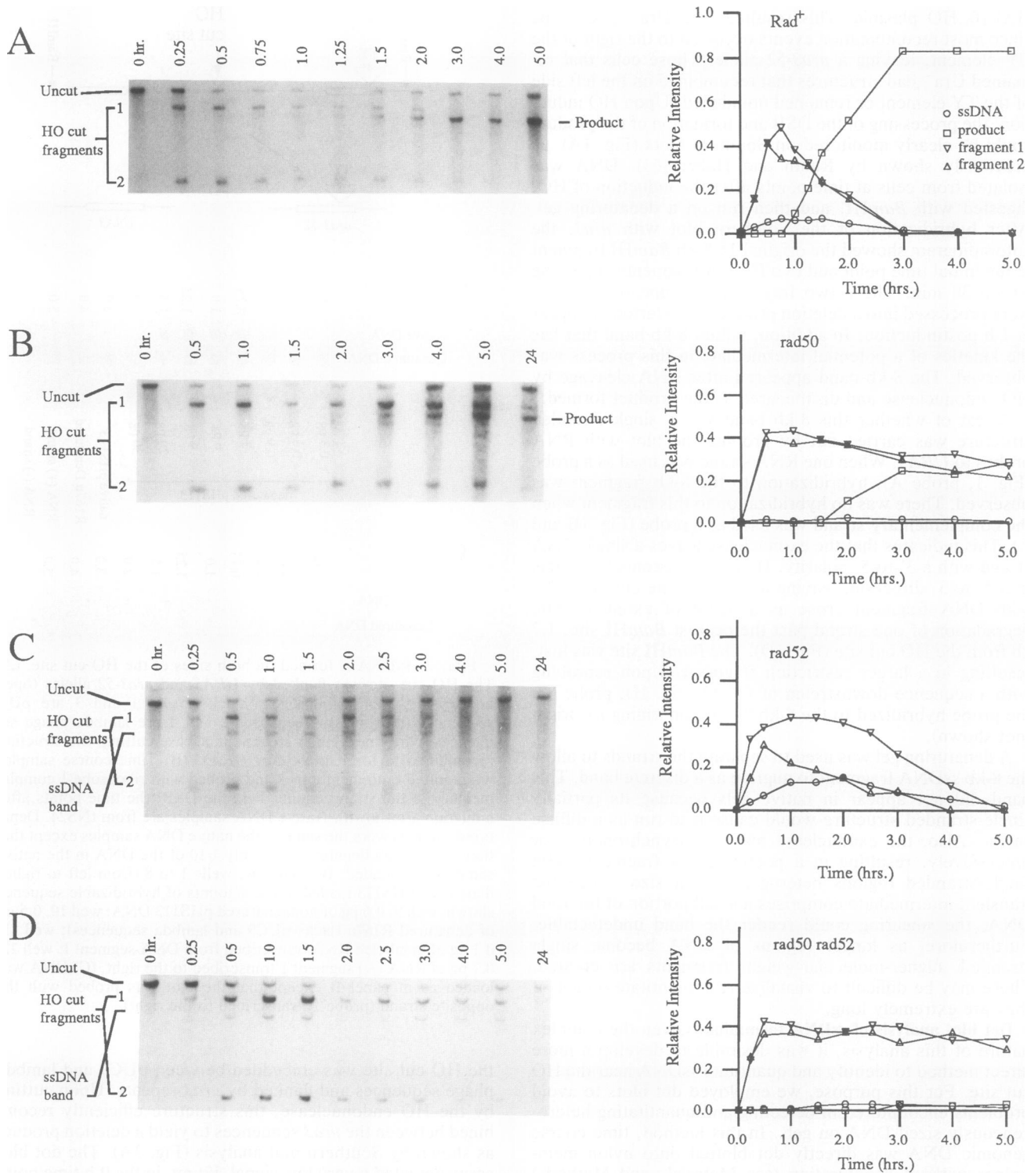

FIG. 3. Kinetics of ssDNA formation. HO endonuclease was induced in four strains: tNS24 (Rad$^+$) (A), tNS313 (*rad50*) (B), tNS418 (*rad52*) (C), and tNS397 (*rad50 rad52*) (D). Each strain has the *ura3* structure shown in Fig. 2. DNA was extracted at the times shown and digested with *Bam*HI, electrophoresed on a denaturing gel, blotted, and probed with the 1.17-kb *ura3* sequence. HO endonuclease-cleaved fragments are 12.8 (1) and 4.3 (2) kb. The *Bam*HI fragment before HO endonuclease cutting (16.8 kb) and the product are also shown. The *rad52* and *rad50 rad52* Southern blots also show the ssDNA band appearing at 10.3 kb (equivalent to the 8-kb band in tNR111 shown in Fig. 1). Mean values of two time courses were plotted. The intensities of the bands were plotted as a fraction of the total intensity per lane. The intensity from the HO-uncut band was divided by two since it included two *ura3* sequences. The amount of ssDNA formed was independently measured by the dot blot assay by using probe 2 (Fig. 2) and plotted on the same graph. When probes 1 and 3 were used (results not shown), hybridization to pSE271::GAL10::HO was taken into account by assuming that the centromere plasmid was present at about 1 copy per cell.

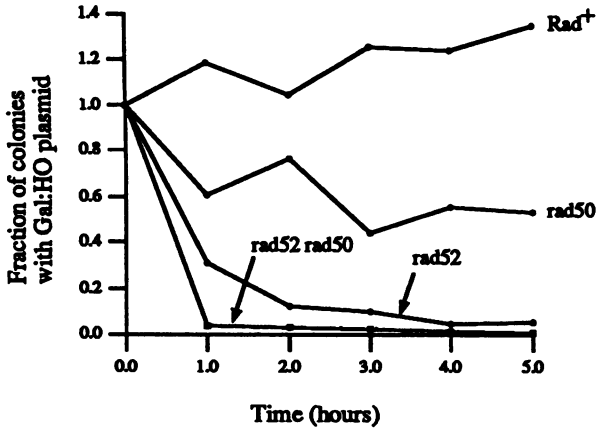

FIG. 4. Cell viability after HO induction. (A) During the time course after the induction of HO, cells were plated on rich medium (YPD). Colonies were replica plated onto selective medium (SD-Trp). Trp^+ cells retained the GAL::HO plasmid. The portion of Trp^+-viable cells relative to the viable cells at the 0-h time point was plotted with respect to time. Rad^+ (tNS24), *rad50* (tNS313 and tNS312), *rad52* (tNS418 and tNS419), and *rad50 rad52* (tNS397) strains were tested.

ssDNA was formed to a comparable extent on the other side of the DSB and with similar kinetics when probe 2 in Fig. 2A was used. The signal was quantitated and plotted on a graph also depicting the loss of the HO-cut fragments and the formation of the product (Fig. 3A). The signal from the 0-h time point of the denatured samples provided a reference point for normalizing signals from different strains. During the course of this reaction, ssDNA composed as much as 8% of the DNA sequence prior to induction (after correcting for the fraction of cells retaining the GAL::HO plasmid). The kinetics of the single-stranded structure were consistent with it being an intermediate of recombination.

We also examined the formation of ssDNA at distances of 1.6 and 2.6 kb away from the HO cut site with the use of probes 3 and 4 (Fig. 2A). We found that ssDNA was formed within a time interval comparable to that seen at positions adjacent to the HO cut site (positions 1 and 2). Any delay in the appearance of ssDNA at a distance of 1.6 kb from the cut site was 15 min or less, the smallest time interval measured.

***rad50* and *rad52* mutations alter DSB-induced recombination.** We also introduced *rad50* and *rad52* gene disruptions into strains with the same *ura3* structure shown in Fig. 2A. When HO was induced in the *rad50* strain, cell viability dropped by 47%, as shown in Fig. 4. Of the survivors, almost all (97%) had recombined and possessed the Ura^- phenotype. Analysis of the DNA structure with Southern blots confirmed that a deletion product was formed (Fig. 3B). Although the HO endonuclease cut efficiently, the overall kinetics leading to product formation were greatly slowed down compared with results with wild-type strains. For example, HO-cleaved fragments were present in the 5-h and the overnight samples, whereas in wild-type strains these disappeared by 3 h. Also, product formation was delayed by 1 to 2 h in the *rad50* strain compared with the wild type. The dot blot assay showed that the production of ssDNA was reduced and slowed down as well. This is shown graphically in relation to the kinetics of the cut fragments and appearance of the deletion product (Fig. 3B).

In the *rad52* strain, induction of HO led to greatly reduced cell viability (95% lethality) (Fig. 4). A Southern blot of the time course DNA showed that very little, if any, mature deletion product was formed (Fig. 3C). The disappearance of the HO-cut fragments is presumed to be due to degradation of ssDNA and/or dsDNA. The dot blot assay showed that a greater amount of ssDNA was produced than in either the wild-type or the *rad50* strain (Fig. 3C, graph). The level of ssDNA reached 20% of the DNA prior to HO induction (after correcting for the fraction of cells retaining the GAL10::HO plasmid). After 2 h, the ssDNA signal level decreased, suggesting that the ssDNA was not protected and was eventually degraded. The loss of ssDNA correlated with the loss of the HO-cut fragments. By using a probe immediately adjacent to the HO cut site on the opposite side (Fig. 2A, probe 1 and data not shown), similar results were obtained.

The differing phenotypes of the *rad50* and *rad52* mutations provided the opportunity to explore their epistatic relationship. Southern blot analysis (Fig. 3D) shows that the *rad50* defect clearly affected the kinetics of recombination in the double mutant. As in the *rad50* mutant, the HO-cut fragments remained for 5 h. Similarly, ssDNA formation, compared with that of the wild type, was reduced when measured with the dot blot assay (Fig. 3D, graph). On the other hand, the data were similar to the *rad52* results in that very little deletion product was formed even after 24 h. We interpret these results to mean that the two *rad* phenotypes are superimposed on each other. The *rad50* defect slows down the formation of ssDNA, and the *rad52* defect prevents the final formation of the deletion product.

With respect to cell viability, the double mutant was similar to the *rad52* single mutant after 5 h of HO induction (Fig. 4). Examination of the survival curves shows that the *rad50 rad52* mutant is less viable than the *rad52* mutant at the 1-h time point. The difference is due to incomplete induction in the *rad52* mutant. Of the Trp^+ colonies at the 1-h time point, 65% were still Ura^+, indicating that induction of recombination had not yet taken place.

Effect of proximity on DSB-induced recombination. The next series of experiments was designed to characterize the process of how the repeated sequences find each other. We asked whether the search process was constrained to choose the two repeated sequences that were closest to the DSB if three copies of *ura3* were provided. Figure 5A shows a structure designed to test this. A plasmid with two copies of *URA3* was integrated at the *ura3-52* locus to yield a structure with three copies of *ura3* (labeled A, B, and C). The HO cut site was situated between copies B and C. In order to give a viable cell upon the induction of HO, copy C must recombine with either copy A or B, resulting in a full or partial deletion product. The relative frequencies of the two products could be determined either phenotypically or by Southern blots. Phenotypically, a Ura^+ or a Ura^- cell results from a partial or a full deletion product, respectively (Fig. 5A). An alternate measurement was made by densitometrically analyzing Southern blots. Cleavage at the *Bgl*II sites resulted in either a 2.9- or a 6.6-kb band, depending on whether the full or partial deletion product was formed. Southern blot analysis also provided confirmation that the galactose induction of HO was successful. Figure 5C, lane tNS130, shows the result of such an induction. The partial deletion product band at 6.6 kb was more intense than the complete deletion band at 2.9 kb. We observed that 91% of the time, the two *ura3* regions closest to the cut site recombined when assayed by colony phenotype (85% by the densitometric assay). This indicates that there is a proximity effect in which the two closest copies find each other and recombine.

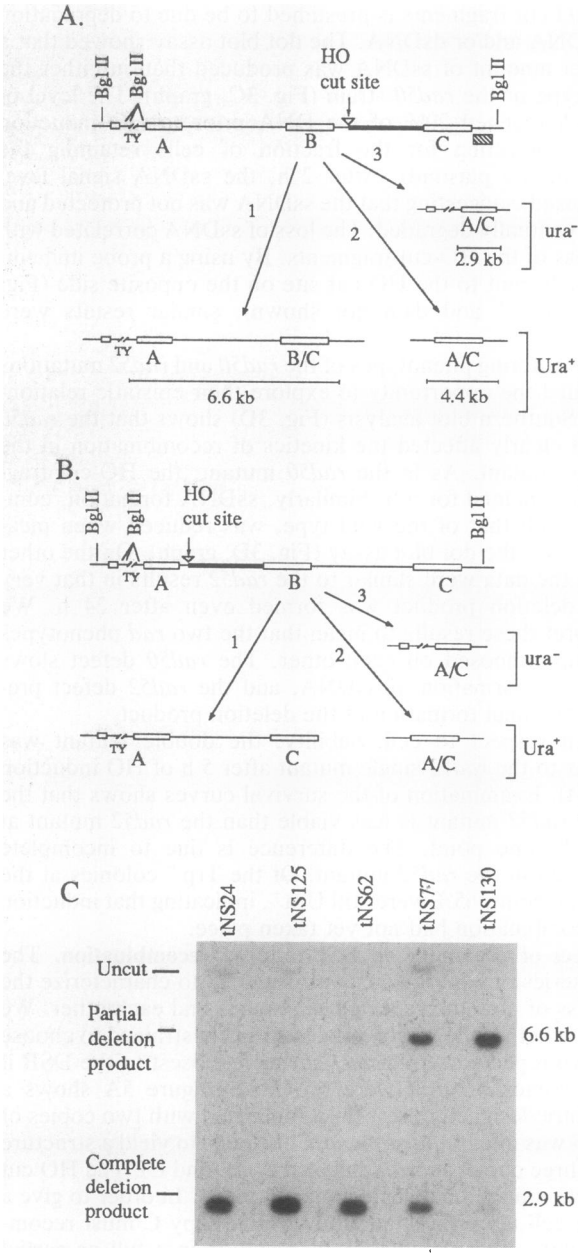

FIG. 5. Repeated sequences nearest the DSB preferentially recombine. (A) Strain tNS130 was constructed with three copies of *ura3* labeled A, B, and C. When HO endonuclease cuts, there are three possible recombinant products: (1) B and C recombine to yield a partial deletion product (Ura^+), (2) A and C recombine so as to remove the TY element (Ura^+), and (3) A and C recombine to give a *ura3-52* allele (Ura^-). The heavy line is lambda phage DNA. *Bgl*II restriction fragments are not drawn to scale. (B) The structure of tNS351 (shown) is a permutation of the *ura3* structure in tNS130. Again, three products are possible: a partial deletion, a complete deletion, and a TY-less recombinant. (C) DNA from HO-induced cultures was digested with *Bgl*II, electrophoresed, blotted, and probed with a downstream sequence (panel A, hatched box). Strains tNS24, tNS125, tNS62, tNS77, and tNS130 have 0, 142, 205, 415, and 1,170 bp, respectively, of *ura3* homology in the middle position (Fig. 6). No signal at 4.4 kb was observed because of the low level of the TY-less product.

We wished to rule out any bias that the TY element in *ura3-52* might confer on recombination. To accomplish this, the *ura3-52* allele was replaced with a *ura3-Nco* allele. The preference for partial deletions was still observed (71% by densitometry). As an additional test, another construction (tNS351) was made where the cut site was placed, near the leftmost *ura3* (copy A) (Fig. 5B). In this permutation, the TY element should not bias which deletion product is formed. The two *ura3* sequences closest to the cut site again recombined most of the time (84% by colony assays and 78% by densitometry). When the *ura3-52* allele was replaced with the *ura3-Nco* allele in this latter structure, partial deletions were formed at a similar frequency (78% by densitometry).

Homology requirements of DSB-induced recombination. The basic structure in Fig. 5A was used to test homology requirements by varying the size of the middle *ura3* sequence (copy B). We wished to determine whether there is a threshold size at which copy C interacts only with A but not B. Figure 6A shows the size and location of the smaller *ura3* segments. A Southern blot of five representative strains with 0, 142, 205, 415, and 1,170 bp of *ura3* sequence in the middle position shows a gradual increase in the partial deletion product (see Fig. 5C). There is an approximately linear dependence of recombination on the length of homology when measured by densitometry or by colony assays (Fig. 6B and C). Above 0.4 kb, the fraction of recombinants using segment B begins to level off as the proportion exceeds 50% of the total events.

We also tested segments of *ura3* that were 30, 63, or 89 bp long to estimate the minimum homology requirements. Frequencies were determined by colony assays since partial deletion products were not detected on Southern blots when testing strains with the 30- and 63-bp alleles. In strains containing the 30-, 63-, or 89-bp alleles, the partial deletion products arose at a low frequency. This made it necessary to distinguish these Ura^+ products from other Ura^+ cells present at a low frequency. Ura^+ colonies can arise from the partial deletion, from uninduced cells, or from recombinants that have lost the TY element (Fig. 5A). These three possibilities were distinguished by testing individual Ura^+ colonies by Southern blots (see Materials and Methods). With the 89-bp strain, 40 colonies with partial deletions were detected among 72 Ura^+ derivatives from a total of 1,515 galactose-induced colonies. The frequency of partial deletions was 2.6%. Southern blot analysis of 43 or 33 Ura^+ colonies from strains containing the 30- or 63-bp alleles revealed no partial deletion products among a total of 1,749 and 1,937 colonies, respectively (less than 0.06%).

Two additional sequences were tested from an internal position (136 bp) and from the 3′ end (262 bp) (in strains tNS228 and tNS262, respectively [Fig. 6A]). Unlike the previous strains, when these recombine to give a partial deletion, the resulting phenotype is Ura^-. Hence, these strains (tNS228 and tNS262) could only be assayed densitometrically with Southern blots. These gave partial deletions at frequencies of 15 and 16%. Since these values are consistent with the above data, the homology dependence does not appear to be due to a phenomenon specific to the 5′ end of the *ura3* sequence.

DISCUSSION

The first part of our investigation focused on the formation of ssDNA at a DSB made by the HO endonuclease. Our results are consistent with ssDNA being a recombination intermediate of this process on the basis of its kinetics and

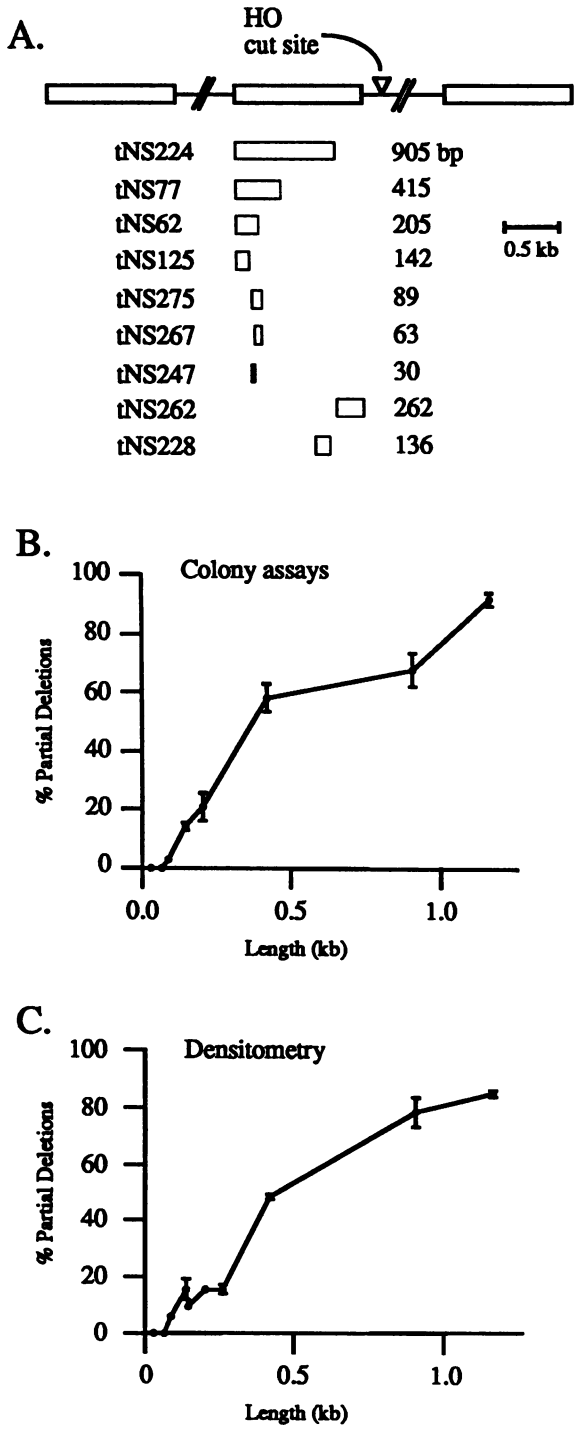

FIG. 6. Homology requirements of DSB-induced recombination. (A) tNS130 (Fig. 5) was constructed with three *ura3* sequences. Other strains were made with smaller segments of *ura3* in the middle position shown with the strain name and the sizes of the middle *ura3* sequence. (B) The portion of deletion products that were partial deletions was plotted against the size of the middle *ura3* sequence. This was measured by colony assays (Ura^+ Trp^+/total Trp^+ colonies) after a 5-h galactose induction. (C) The frequency of partial deletions was also determined by densitometry of Southern blots. The fraction of partial deletion products is the intensity of the partial deletion product divided by the sum of intensities of the partial and complete deletion products. The standard deviations and means of three to seven measurements were plotted.

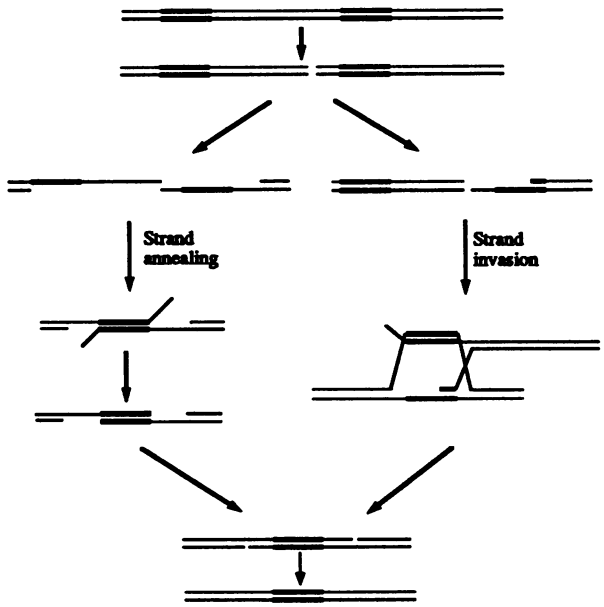

FIG. 7. Recombination models. In the single-strand annealing model, an exonuclease degrades one strand to expose complementary sequences (dark lines) on each side of the DSB. After complementary sequences anneal to form one double-stranded sequence, the single-stranded tails are degraded by a nuclease. DNA polymerase and ligase complete the process. In the strand invasion model, DNA from one repeat invades the duplex DNA on the other side of the break to form heteroduplex DNA. Strand invasion may be preceded by ssDNA degradation to expose one of the repeats or by dsDNA degradation to enlarge the gap (not shown). Other nucleases degrade the ssDNA tails and act to resolve the crossover structure.

the effect that *rad50* and *rad52* have on its rate of formation. ssDNA has a postulated role as an intermediate in a number of recombination models (24, 32, 46, 73, 75). We view the role of ssDNA within the framework of two models. The single-strand annealing model proposes that single-stranded regions are formed on both sides of the DSB and that the repeated sequences anneal with each other (Fig. 7) (32). The resulting structure is subsequently processed into the recombined product. This model is supported by the analysis of products of DNA transformation experiments (12, 32), by monitoring the fate of DNA injected into *Xenopus* oocytes (11, 39–41), and by the analysis of the kinetics of DSB-induced recombination products in *S. cerevisiae* (16).

Recombination may also occur in part by a strand invasion mechanism (Fig. 7). In this model, a single-stranded region forms on at least one side of the DSB. One strand invades the homologous duplex region on the opposite side and forms a Holliday junction that is resolved to give a recombined product. In some respects, this is similar to HO-induced recombination events at *MAT*, in which one side of the DSB is apparently protected from single-stranded degradation by the presence of the silent cassettes (78). The single-stranded tail invades the homologous sequence of the *HML* cassette and thus initiates recombination. Although ssDNA in our experiments is formed on both sides of the DSB, consistent with the single-strand annealing model, it is still possible that a strand invasion pathway may contribute to recombination between repeated sequences.

With respect to ssDNA formation, the process can be broadly broken down into two steps. In the first step, ssDNA forms as a result of the action of one or more exonucleases.

The second step consists of the processing of the ssDNA-dsDNA structure to form a recombined product. The processing includes the removal of the 3′ tails from either the annealed structure (strand annealing model) or a crossover structure (Holliday junction in the strand invasion model). Both steps affect the overall rate of the recombination process. The appearance of the ssDNA depends on the relative rates of both steps.

***rad50* and *rad52*.** Our results confirm that DSBs induced in a *rad52* background are lethal to the extent that 95% of the cells with DSBs died. Southern blot analyses show that only a small fraction, if any, of the DSBs are repaired by recombination after 5 h. Furthermore, a greater amount of ssDNA is formed in the *rad52* strain than in the wild-type strain. There are two interpretations of this data. The first proposes that there is a recombinational block subsequent to the action of an exonuclease. This block would prevent the repair of the DSB and lead to an accumulation of ssDNA. One possible block might be the failure to form a strand invasion structure in *rad52* strains as shown in mating type switching experiments (78). The second interpretation contends that in wild-type strains the *RAD52*-dependent activity slows down or limits the exonucleolytic activity by partially protecting the end of the dsDNA. For example, lack of a DNA "capping" protein in *rad52* mutants would permit an exonuclease to more rapidly digest one strand of the DNA. The *rad52* defect may affect both the exonucleolytic step and one or more subsequent steps in recombination. The distinction between these two interpretations is being investigated.

Although a DSB has a predominantly lethal effect in *rad52* strains, there are some situations in which DSBs can be repaired in a *rad52* background. For example, the HO cut site was efficiently repaired when embedded in the tandemly arrayed rDNA cluster or to a lesser extent in *CUP1* arrays (50). The DSB was also repaired about 10% of the time when located within a duplicated *lacZ* sequence (16, 51). These results may mean that the *rad52* mutants retain a reduced ability to find homologous sequences. In the rDNA array, this deficiency may be compensated for by the large number of homologous rDNA units. In the case of *lacZ* duplications, the greater success in repairing the DSB may be due to the close proximity of the homologous sequences to the HO cut site or the larger amount of homologous *lacZ* sequence (compared with *ura3*). In a similar vein, two recombination-defective mutants (*recBC* of *Escherichia coli* and *46* of T4) possessed reduced recombination frequencies and a diminished dependence on homologous length when compared with wild type (67, 69).

The *rad50* mutant presented a very different phenotype. The ssDNA dot blot assay showed that less ssDNA was produced after HO induction. This can be due to either a slower formation of ssDNA or to a faster processing of the DSB (or more precisely, a faster degradation of the 3′ tails). The first explanation is consistent with the slower formation of product and with the persistence of HO-cut fragments throughout the time course. A 5′-to-3′ exonucleolytic activity would normally lead to an apparent loss of HO-cut bands due to the smearing of bands or to the formation of higher-molecular-weight fragments as a result of the inability of *Bam*HI to cleave ssDNA. Either reason would cause the loss of discrete HO-cut bands, such as is seen in *rad52* but not *rad50* mutants. Hence, *rad50* mutants appear to be defective before or at the point of exonucleolytic activity. *rad52*, on the other hand, appears to act later, since the HO-cut fragments disappear yet a mature recombination product fails to appear in a significant amount. It remains a possibility that *rad50* and *rad52* may act at approximately the same stage, if both affect the relative vulnerability of the DNA to nucleases.

During meiosis, *rad50* null mutants fail to form DSBs at sites associated with two recombination hot spots (10, 72). Mutants with the *rad50S* allele produce DSBs but do not exhibit the 5′-to-3′ exonucleolytic degradation present in Rad^+ strains (4, 10, 72). In view of the effect of *rad50* on recombination and on the formation of synaptonemal complexes, it was proposed that *RAD50* might have a role in the search for chromosomal homology (4). In our experiments, we have shown that *rad50* null mutants displayed a reduced exonucleolytic activity and that *rad50* acted at or before the exonucleolytic step. This may correlate with the lack of exonucleolytic activity in *rad50S* and possibly in *rad50* null mutants during meiosis. It is possible that the residual activity we observed is due to partial exposure of the DNA to exonucleolytic activity during the homology search or due to a *rad50*-independent exonuclease present in vegetative cells.

A significant difference between the meiotic defect of *rad50S* and the *rad50* null mutant in HO-induced mitotic cells is that the latter can complete recombination. Even though the mitotic recombination process is slowed down in *rad50* mutants, mature recombination products can be seen on the Southern blots and cell survival was measured at 53%. The slowed recombination kinetics and weak lethality of *rad50* offers an explanation of certain other *rad50* phenotypes. It is consistent with the observation that *rad50* mutants are among the mutants less sensitive to ionizing radiation in the *rad52* epistasis group. A *rad50* mutant to some extent would be able to repair a single lesion but probably could not survive multiple lesions produced at higher dosages. One DSB per genome is inflicted by about 1 to 2 kilorads of ionizing irradiation (58), and *rad50* mutants display a minimal sensitivity to ionizing radiation at this level (44). The limited ability to repair a DSB might also explain results indicating that mating type switching was not strongly affected in *rad50* HO strains (36). A preliminary experiment employing the GAL::HO fusion indicated that HO endonuclease cleavage at *MAT* led to cell death at a frequency comparable to that seen in this study at *URA3* in a *rad50* strain (79).

Relationship between *rad50* and *rad52*. Conventional epistasis analysis usually considers the effect of one phenotype such as cell death upon irradiation. This type of analysis relies upon the ability to discern an additive or synergistic effect in the double mutant. The viability study presented in Fig. 4 agrees with the observation that *rad52* is epistatic to *rad50*, as seen previously in irradiation studies (44). However, our data are not accurate enough to see an additive contribution to inviability in the double mutant.

The Southern blot analyses provide us with a more detailed view of the events leading up to the inviability of the double mutant. The analysis of single mutants shows us that *rad50* is a partial block to recombination whereas *rad52* is a strong block. These blocks are maintained in the double mutant to the extent that *rad52* prevents formation of the product that normally would have appeared in the single *rad50* mutant. The double mutant thus exhibits a level of cell death equal to or greater than that associated with the *rad52* mutant alone.

An examination of Southern blots of the single mutants suggests that *rad50* acts before or at the exonucleolytic step and *rad52* acts later (discussed above). Since we are seeing the combined characteristics of *rad50* and *rad52* in the

double mutant, one might also expect to find an intermediate level of ssDNA formation. For example, ssDNA would be generated more slowly because of the *rad50* defect, but it might accumulate because of the *rad52* block. Unfortunately, our data are unclear on this point because there is a discrepancy between the significant accumulation of the ssDNA *Bam*HI band and the less-intense signal from the dot blot analysis (Fig. 3D). We do not understand this difference but hypothesize that the difference may be explained in part by the fact that a probe very close to the HO cut site was used to monitor the dot blots while a more distant probe was used to examine the restriction fragments. If in the *rad50 rad52* double mutant the 3′ end is also subject to degradation, the amount of ssDNA detected by the dot blots would be underestimated. Regardless of the level of ssDNA formation, the kinetics of the HO-cut fragments and the absence of product support the proposal that *rad50* acts before *rad52*.

Proximity effect. We showed that there was a distinct proximity effect in that the copies of *ura3* nearest to the DSB were used preferentially. This result is consistent with an orderly searching process in which sequences adjacent to the DSB on one side are compared with sequences on the other side until a homologous match is found. In the single-strand annealing model, for example, single-stranded regions nearest the DSB may be compared first and then sequences farther away may be compared as an exonuclease moves down the DNA strands. A similar picture can be drawn for the strand invasion model, in which an ssDNA-dsDNA complex is formed as a component of the homology search. For example, the *recA* protein in vitro promotes the formation of triplexes that are thought to be intermediates of the homology search (6). In either the strand annealing model or the invasion model, a sliding mechanism would result in a proximity effect.

Alternatively, one can envision a stochastic process in which sequences on each side of the DSB are randomly tested with sequences on the other side. This is similar to the diffusion model supported by studies of the *recA* protein in vitro (18, 19). In our experiments, sequences close to the DSB would preferentially recombine because they have a smaller volume to search. The proximity effect may also suggest that there is a chromosomal constraint on the mobility of a repeated sequence that limits its ability to find distant sequences.

Homology requirements. DSB-induced recombination between chromosomal repeats was linearly dependent on the length of homology and appeared to have a minimum homology requirement in the competition experiments we devised. There was a threshold length between 63 and 89 bp below which recombination occurred at such a low level that it could not be detected if it occurred at all. This threshold represents the minimal length needed for efficient recombination. This requirement may reflect the length needed for a sequence to search and find its homologous sequence, or it may be the length needed to form a stable intermediate structure such as a DNA-protein complex. In reference to spontaneous recombination, Shen and Huang proposed that this minimum-length unit possesses a fixed recombination frequency (67). Increasing the number of such units by increasing the total length of homology causes a proportional increase in the overall recombination frequency. Hence, the overall frequency of recombination becomes linearly dependent on the length of homology. This model would also account for our observations that DSB-induced recombination is approximately linear over the range of 0.089 to 0.4 kb. Presumably, a maximum recombination value will be reached as longer lengths are used. This is reflected in a slight leveling off of the curve seen above 0.4 kb as the maximum value is approached.

ACKNOWLEDGMENTS

We thank C. White, H. Sun, B. Ray, J. Fishman-Lobell, M. Lichten, and J. J. Kupiec for reading our manuscript and the Rosbash and Szostak labs for use of their β scanners.

This work was supported by NIH grants GM20056 and by NSF grant DCB8711517.

REFERENCES

1. **Adzuma, K., T. Ogawa, and H. Ogawa.** 1984. Primary structure of the *RAD52* gene in *Saccharomyces cerevisiae*. Mol. Cell. Biol. **4**:2735–2744.
2. **Ahn, B. Y., K. J. Dornfeld, T. J. Fagrelius, and D. M. Livingston.** 1988. Effect of limited homology on gene conversion in a *Saccharomyces cerevisiae* plasmid recombination system. Mol. Cell. Biol. **8**:2442–2448.
3. **Alani, E., L. Cao, and N. Kleckner.** 1987. A method for gene disruption that allows repeated use of *URA3* selection in the construction of multiply disrupted yeast strains. Genetics **116**: 541–545.
4. **Alani, E., R. Padmore, and N. Kleckner.** 1990. Analysis of wild-type and *rad50* mutants of yeast suggests an intimate relationship between meiotic chromosome synapsis and recombination. Cell **61**:419–436.
5. **Ayares, D., L. Chekuri, K.-Y. Song, and R. Kucherlapati.** 1986. Sequence homology requirements for intermolecular recombination in mammalian cells. Proc. Natl. Acad. Sci. USA **83**:5199–5203.
6. **Bianchi, M., C. DasGupta, and C. M. Radding.** 1983. Synapsis and the formation of paranemic joints by *E. coli RecA* protein. Cell **34**:931–939.
7. **Boeke, J. D., F. Lacroute, and G. R. Fink.** 1984. A positive selection for mutants lacking orotidine-5′-phosphate decarboxylase activity in yeast: 5-fluoro-orotic acid resistance. Mol. Gen. Genet. **197**:345–346.
8. **Borts, R. H., M. Lichten, and J. E. Haber.** 1986. Analysis of meiosis-defective mutations in yeast by physical monitoring of recombination. Genetics **113**:551–567.
9. **Budd, M., and R. K. Mortimer.** 1982. Repair of double-strand breaks in a temperature conditional radiation-sensitive mutant of *Saccharomyces cerevisiae*. Mutat. Res. **103**:19–26.
10. **Cao, L., E. Alani, and N. Kleckner.** 1990. A pathway for generation and processing of double-strand breaks during meiotic recombination in *Saccharomyces cerevisiae*. Cell **61**:1089–1102.
11. **Carroll, D., S. H. Wright, R. K. Wolff, E. Grzesiuk, and E. B. Maryon.** 1986. Efficient homologous recombination of linear DNA substrates after injection into *Xenopus laevis* oocytes. Mol. Cell. Biol. **6**:2052–2062.
12. **Chakrabarti, S., and M. M. Seidman.** 1986. Intramolecular recombination between transfected repeated sequences in mammalian cells is nonconservative. Mol. Cell. Biol. **6**:2520–2526.
13. **Church, G. M., and W. Gilbert.** 1984. Genomic sequencing. Proc. Natl. Acad. Sci. USA **81**:1991–1995.
14. **Feinberg, A. P., and B. Vogelstein.** 1984. A technique for radiolabelling DNA restriction endonuclease fragments to high specific activity. Anal. Biochem. **137**:266–267. (Addendum.)
15. **Fishman-Lobell, J., and J. E. Haber.** Unpublished data.
16. **Fishman-Lobell, J., N. Rudin, and J. E. Haber.** 1991. Submitted for publication.
17. **Game, J. C., K. C. Sitney, V. E. Cook, and R. K. Mortimer.** 1989. Use of a ring chromosome and pulsed-field gels to study interhomolog recombination, double-strand DNA breaks and sister-chromatid exchange. Genetics **123**:695–713.
18. **Gonda, D. K., and C. M. Radding.** 1983. By searching processively *RecA* protein pairs DNA molecules that share a limited stretch of homology. Cell **34**:647–654.
19. **Gonda, D. K., and C. M. Radding.** 1986. The mechanism of the

search for homology promoted by *recA* protein: facilitated diffusion within nucleoprotein networks. J. Biol. Chem. **261:** 13087–13096.
20. **Gottlieb, S., J. Wagstaff, and R. E. Esposito.** 1989. Evidence for two pathways of meiotic intrachromosomal recombination in yeast. Proc. Natl. Acad. Sci. USA **86:**7072–7076.
21. **Haber, J. E., and P. Thorburn.** 1984. Healing of broken linear dicentric chromosomes in yeast. Genetics **106:**207–226.
22. **Hill, A., and K. Bloom.** 1989. Acquisition and processing of a conditional dicentric chromosome in *Saccharomyces cerevisiae*. Mol. Cell. Biol. **9:**1368–1370.
23. **Hoekstra, M. F., T. Naughton, and R. E. Malone.** 1986. Properties of spontaneous mitotic recombination occurring in the presence of the *rad52-1* mutation of *Saccharomyces cerevisiae*. Genet. Res. **48:**9–17.
24. **Holliday, R.** 1964. A mechanism for gene conversion in fungi. Genet. Res. **5:**282–304.
25. **Ito, H., Y. Fukuda, K. Murata, and A. Kimura.** 1983. Transformation of intact yeast cells treated with alkali cations. J. Bacteriol. **153:**163–168.
26. **Jackson, J. A., and G. R. Fink.** 1981. Gene conversion between duplicated genetic elements in yeast. Nature (London) **292:**306–311.
27. **Klar, A. J., J. N. Strathern, and J. A. Abraham.** 1984. Involvement of double-strand chromosomal breaks for mating-type switching in *Saccharomyces cerevisiae*. Cold Spring Harbor Symp. Quant. Biol. **49:**77–88.
28. **Klein, H.** 1988. Different types of recombination events are controlled by the *RAD1* and *RAD52* genes of *Saccharomyces cerevisiae*. Genetics **120:**367–377.
29. **Kolodkin, A. L., A. J. S. Klar, and F. W. Stahl.** 1986. Double-strand breaks can initiate meiotic recombination in *S. cerevisiae*. Cell **46:**733–740.
30. **Kostriken, R., and F. Heffron.** 1984. The product of the HO gene is a nuclease: purification and characterization of the enzyme. Cold Spring Harbor Symp. Quant. Biol. **49:**89–104.
31. **Kostriken, R., J. N. Strathern, A. J. Klar, J. B. Hicks, and F. Heffron.** 1983. A site-specific endonuclease essential for mating-type switching in *Saccharomyces cerevisiae*. Cell **35:**167–174.
32. **Lin, F.-L., K. Sperle, and N. Sternberg.** 1984. Model for homologous recombination during transfer of DNA into mouse L cells: role for DNA ends in the recombination process. Mol. Cell. Biol. **4:**1020–1034.
33. **Liskay, R. M., A. Letsou, and J. L. Stachelek.** 1987. Homology requirement for efficient gene conversion between duplicated chromosomal sequences in mammalian cells. Genetics **115:**161–168.
34. **Liskay, R. M., J. L. Stachelek, and A. Letsou.** 1984. Homologous recombination between repeated chromosomal sequences in mouse cells. Cold Spring Harbor Symp. Quant. Biol. **49:**183–189.
35. **Malone, R., and R. E. Esposito.** 1980. The *RAD52* gene is required for homothallic interconversion of mating-types and spontaneous recombination in yeast. Proc. Natl. Acad. Sci. USA **77:**503–507.
36. **Malone, R. E.** 1983. Multiple mutant analysis of recombination in yeast *Saccharomyces cerevisiae*. Mol. Gen. Genet. **189:**405–412.
37. **Malone, R. E., and R. E. Esposito.** 1981. Recombinationless meiosis in *Saccharomyces cerevisiae*. Mol. Cell. Biol. **1:**891–901.
38. **Malone, R. E., B. A. Montelone, C. Edwards, K. Carney, and M. F. Hoekstra.** 1988. A reexamination of the *RAD52* gene in spontaneous mitotic recombination. Curr. Genet. **14:**211–223.
39. **Maryon, E., and D. Carroll.** 1989. Degradation of linear DNA by a strand-specific exonuclease activity in *Xenopus laevis* oocytes. Mol. Cell. Biol. **9:**4862–4871.
40. **Maryon, E., and D. Carroll.** 1991. Characterization of recombination intermediates from DNA injected into *Xenopus laevis* oocytes: evidence for a nonconservative mechanism of homologous recombination. Mol. Cell. Biol. **11:**3278–3287.
41. **Maryon, E., and D. Carroll.** 1991. Involvement of single-stranded tails in homologous recombination of DNA injected into *Xenopus laevis* oocyte nuclei. Mol. Cell. Biol. **11:**3268–3277.
42. **McDonnel, M. W., M. N. Simon, and F. W. Studier.** 1977. Analysis of restriction fragments of T7 DNA and determination of molecular weights by electrophoresis in neutral and alkaline gels. J. Mol. Biol. **110:**119–146.
43. **McGill, C., B. Shafer, and J. N. Strathern.** 1989. Co-conversion of flanking sequences with homothallic switching. Cell **57:**459–467.
44. **McKee, R. H., and C. W. Lawrence.** 1980. Genetic analysis of γ-ray mutagenesis in yeast. III. Double-mutant strains. Mutat. Res. **70:**37–48.
45. **Melton, D. A., P. A. Krieg, M. R. Rebagliati, T. Maniatis, K. Zinn, and M. R. Green.** 1984. Efficient *in vitro* synthesis of biologically active RNA and RNA hybridization probes from plasmids containing a bacteriophage SP6 promoter. Nucleic Acids Res. **12:**7035–7056.
46. **Meselson, M. S., and C. M. Radding.** 1975. A general model for genetic recombination. Proc. Natl. Acad. Sci. USA **72:**358–361.
47. **Nickoloff, J. A., E. Y. Chen, and F. Heffron.** 1986. A 24-base-pair DNA sequence from the *MAT* locus stimulates intergenic recombination in yeast. Proc. Natl. Acad. Sci. USA **83:**7831–7835.
48. **Nickoloff, J. A., J. D. Singer, M. F. Hoekstra, and F. Heffron.** 1989. Double-strand breaks stimulate alternative mechanisms of recombination repair. J. Mol. Biol. **207:**527–541.
49. **Orr-Weaver, T. L., J. W. Szostak, and R. J. Rothstein.** 1981. Yeast transformation: a model system for the study of recombination. Proc. Natl. Acad. Sci. USA **78:**6354–6358.
50. **Ozenberger, B. A., and G. S. Roeder.** 1991. A unique pathway of double-strand break repair operates in tandemly repeated genes. Mol. Cell. Biol. **11:**1222–1231.
51. **Plessis, A., A. Perrin, J. E. Haber, and B. Dujon.** Genetics, in press.
52. **Prakash, L., and P. Taillon-Miller.** 1981. Effects of the *rad52* gene on sister chromatid recombination in *Saccharomyces cerevisiae*. Curr. Genet. **3:**247–250.
53. **Prakash, S., L. Prakash, W. Burke, and B. A. Monteleone.** 1980. Effects of the *RAD52* gene on recombination in *Saccharomyces cerevisiae*. Genetics **94:**31–50.
54. **Raveh, D., S. H. Hughes, B. K. Shafer, and J. N. Strathern.** 1989. Analysis of the HO-cleaved *MAT* DNA intermediate generated during the mating type switch in the yeast *Saccharomyces cerevisiae*. Mol. Gen. Genet. **220:**33–42.
55. **Ray, A., N. Machin, and F. W. Stahl.** 1989. A DNA double chain break stimulates triparental recombination in *Saccharomyces cerevisiae*. Proc. Natl. Acad. Sci. USA **86:**6225–6229.
56. **Ray, A., I. Siddiqi, A. L. Kolodkin, and F. W. Stahl.** 1988. Intra-chromosomal gene conversion induced by a DNA double-strand break in *Saccharomyces cerevisiae*. J. Mol. Biol. **201:** 247–260.
57. **Resnick, M. A.** 1975. The repair of double strand breaks in DNA: a model involving recombination. J. Theor. Biol. **59:**97–106.
58. **Resnick, M. A., and P. Martin.** 1976. The repair of double-strand breaks in the nuclear DNA of *Saccharomyces cerevisiae* and its genetic control. Mol. Gen. Genet. **143:**119–129.
59. **Rickey, C.** 1990. Efficient electroporation of yeast. Mol. Biol. Rep. **9:**2–3.
60. **Rose, M., P. Grisafi, and D. Botstein.** 1984. Structure and function of the yeast *URA3* gene: expression in *Escherichia coli*. Gene **29:**113–124.
61. **Rose, M., and F. Winston.** 1984. Identification of a Ty insertion within the coding sequence of the *S. cerevisiae URA3* gene. Mol. Gen. Genet. **193:**557–560.
62. **Rubnitz, J., and S. Subramani.** 1984. The minimum amount of homology required for homologous recombination in mammalian cells. Mol. Cell. Biol. **4:**2253–2258.
63. **Rudin, N., and J. E. Haber.** 1988. Efficient repair of HO-induced chromosomal breaks in *Saccharomyces cerevisiae* by recombination between flanking homologous sequences. Mol. Cell. Biol. **8:**3918–3928.
64. **Rudin, N., E. Sugarman, and J. E. Haber.** 1989. Genetic and

physical analysis of double-strand break repair and recombination in *Saccharomyces cerevisiae*. Genetics **122**:519–534.

65. **Schild, D., B. Konforti, C. Perez, W. Gish, and R. Mortimer.** 1983. Isolation and characterization of yeast DNA repair genes. I. Cloning of the *RAD52* gene. Curr. Genet. **7**:85–92.
66. **Seth, A.** 1984. A new method for linker ligation. Gene Anal. Tech. **1**:99–103.
67. **Shen, P., and H. V. Huang.** 1986. Homologous recombination in *Escherichia coli*: dependence on substrate length and homology. Genetics **112**:441–457.
68. **Sherman, F., G. R. Fink, and J. B. Hicks.** 1983. Methods in yeast genetics. Cold Spring Harbor Laboratory, Cold Spring Harbor, N.Y.
69. **Singer, B. S., L. Gold, P. Gauss, and D. H. Doherty.** 1982. Determination of the amount of homology required for recombination in bacteriophage T4. Cell **31**:25–33.
70. **Strathern, J. N., A. J. Klar, J. B. Hicks, J. A. Abraham, J. M. Ivy, K. A. Nasmyth, and C. McGill.** 1982. Homothallic switching of yeast mating type cassettes is initiated by a double-stranded cut in the *MAT* locus. Cell **31**:183–192.
71. **Sun, H., D. Treco, N. P. Schultes, and J. W. Szostak.** 1989. Double-strand breaks at an initiation site for meiotic gene conversion. Nature (London) **338**:87–90.
72. **Sun, H., D. Treco, and J. W. Szostak.** 1991. Extensive 3′-overhanging, single-stranded DNA associated with the meiosis-specific double-strand breaks at the *ARG4* recombination initiation site. Cell **64**:1155–1161.
73. **Szostak, J. W., W. T. L. Orr, R. J. Rothstein, and F. W. Stahl.** 1983. The double-strand-break repair model for recombination. Cell **33**:25–35.
74. **Viret, J.-F., and J. C. Alonso.** 1987. Generation of linear multigenome-length plasmid molecules in *Bacillus subtilis*. Nucleic Acids Res. **15**:6349–6367.
75. **Wake, C., F. Vernaleone, and J. H. Wilson.** 1985. Topological requirements for homologous recombination among DNA molecules transfected into mammalian cells. Mol. Cell. Biol. **5**:2080–2089.
76. **Watt, V. M., C. J. Ingles, M. S. Urdea, and W. J. Rutter.** 1985. Homology requirements for recombination in *Escherichia coli*. Proc. Natl. Acad. Sci. USA **82**:4768–4772.
77. **Weiffenbach, B., and J. E. Haber.** 1981. Homothallic mating type switching generates lethal breaks in *rad52* strains of *Saccharomyces cerevisiae*. Mol. Cell. Biol. **6**:522–534.
78. **White, C. I., and J. E. Haber.** 1990. Intermediates of recombination during mating type switching in *Saccharomyces cerevisiae*. EMBO J. **9**:663–673.
79. **White, C. I., and J. E. Haber.** Unpublished data.
80. **Yuan, L.-W., and R. L. Keil.** 1990. Distance-independence of mitotic intrachromosomal recombination in *Saccharomyces cerevisiae*. Genetics **124**:263–273.
81. **Zamb, T. J., and T. D. Petes.** 1981. Unequal sister-strand recombination within yeast ribosomal DNA does not require the *RAD52* gene product. Curr. Genet. **3**:125–132.